Proceedings of the 2nd World Congress on Civil, Structural, and Environmental Engineering (CSEE'17)
Barcelona, Spain – April 2 – 4, 2017
Paper No. ICSENM 139
ISSN: 2371-5294
DOI: 10.11159/icsenm17.139

Quasi-static Loading Test of Confined Clay Brick Masonry Walls Retrofitted with Post-tensioned Tendons

Hang Liu, Shaofeng Hua, Chunguang Lan, Xuezhong Yang
Beijing Building Construction Research Institute
No.34, Fuxing Road, Haidian District, Beijing, P. R. China
liuhang71@sina.com, 58481680@qq.com, 2368096@qq.com, 99883730@qq.com

Abstract **-** In this paper, the test results of eight confined clay brick masonry walls retrofitted using externally post-tensioned tendons and subjected to reversed in-plane quasi-static cyclic loadings are presented. One wall was built as a non-retrofitted wall, and the remaining seven were retrofitted using post-tensioned high strength steel strands. Five magnitudes of axial force ratio and three spacing of tendons were investigated. A complete description of the test setup and results is provided, including the design and construction of the walls, the damage patterns, the shear capacity, the lateral deformation and the equivalent viscous damping coefficient. Test results show that the mechanical behaviors and the failure patterns of the retrofitted walls could be significantly improved. The in-plane shear capacity of the post-tensioned brick walls observed ranged from 1.28 to 2.11 times the shear capacity of the non-retrofitted wall, and the ductility index ranged from 1.33 to 3.8 times the ductility index of the non-retrofitted wall. Finally, a simple analysis method is presented for prediction of shear capacity.

Keywords**:** Masonry wall; Clay brick; Seismic retrofitting; Post-tensioning; Quasi-static loading test; Shear capacity

1. Introduction

Currently, brick masonry structure is one of the most widely used structures all over the world. It was estimated that more than 70% of the buildings inventory worldwide is masonry buildings[1]. Experiences show that the collapse ratio of brick masonry building is very high during a strong earthquake. In the Sichuan earthquake occurred in 2008, a lot of clay brick masonry buildings collapsed or suffered serious damage. In recent years, post-tensioned tendons have been used to improve the seismic behaviors and the out of plane behaviors of masonry structure in some countries[2-12]. It was shown that the in plane shear capacity, the out of plane flexural capacity, the ductility and the energy dissipation capability of brick masonry structure retrofitted with post-tensioned tendons were significantly improved, thereby the seismic performance was greatly enhanced. However in China, few studies on seismic retrofitting of masonry walls with post-tensioned tendons have been carried out, not to mention practical application[13-15].

In this paper, the test results of 8 confined clay brick masonry walls subjected to reversed in-plane quasi-static cyclic loadings are presented, including seven retrofitted walls using externally post-tensioned tendons and one non-retrofitted wall. The results of the retrofitted walls were compared with that of the non-retrofitted one to validate the feasibility of the retrofitting method with post-tensioned technology.

2. Design of the walls and test setup

The length, height and thickness of the test walls are 3.6m, 2.8m and 0.24m, respectively. The outline dimensions of the test walls are shown in Fig. 1. The main test parameters of the walls, including the spacing of the post-tensioned tendons and the magnitudes of the prestressing forces are shown in Table 1. The wall W1 is the non-retrofitted wall and the walls W2~W8 are retrofitted walls with post-tensioned tendons. The bricks of the test walls are the most commonly used bricks in China, with the size of 240mm × 115mm × 53mm and the brick's characteristic compressive strength f_1 is 10MPa. The mortar's characteristic compressive strength f_2 is 7.5MPa.

Table 1: Test wall specifications.

Test Wall	f_1 (MPa)	f_2 (MPa)	Major parameters of prestressing tendons			
			Quantity (pairs)	σ_{p0}/f *	Spacing （mm）	Prestressing force （kN）
W1	10	7.5	--	--	--	--
W2			3	0.15	1200	36.5
W3			4	0.3	900	54.8
W4			5	0.15	720	21.9
W5			4	0.15	900	27.4
W6			4	0.2	900	36.5
W7			4	0.4	900	73
W8			4	0.5	900	91.3

*σ_{p0} is the axial stress of the masonry wall due to prestress. f is the masonry crushing strength, which can be calculated as follows[16]:

$$f = 0.78 f_1^{0.5}(1+0.07 f_2) \tag{1}$$

Where, f_1 is the characteristic compressive strength of brick and f_2 is the characteristic compressive strength of mortar.

The test walls are composed of concrete foundation beam, top beam, tie columns and clay brick masonry. The tie columns was cast after the construction of the brick wall. The sizes and the reinforcements of the concrete foundation beam, top beam and the tie columns are shown in Fig 2. The average compressive strength of concrete cube of the tie columns and the top beam is 31.42MPa. The diameter of the post-tensioned tendons is 15.24mm and the tensile strength is 1,860 MPa. The post-tensioning tendons were installed as external tendons in pairs at both sides of the walls, with fixed end anchored in the foundation beam and tensioning end anchored on the top beam. The locations of the tendons are shown in Fig.1 and the spacing of the tendons are listed in Table 1.

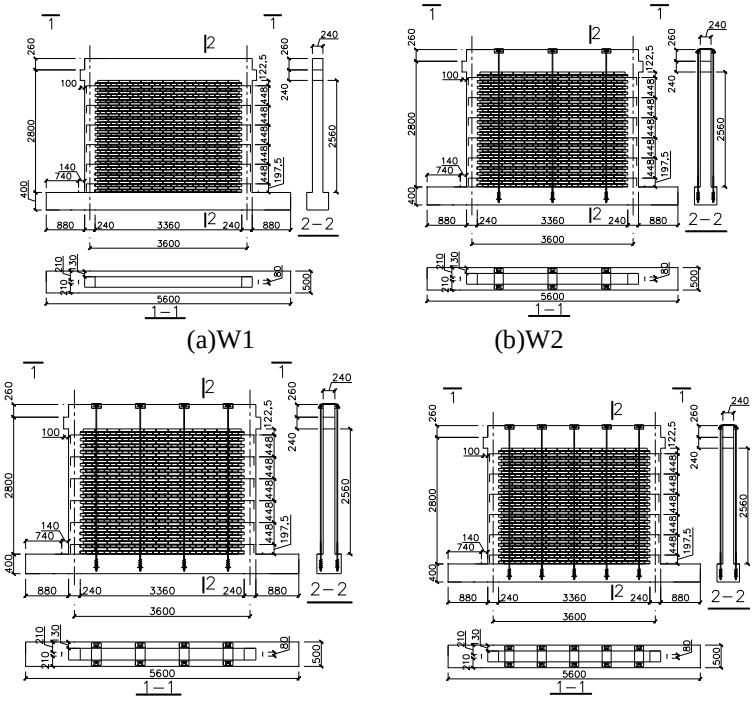

(a)W1 (b)W2

(c)W3,W5,W6,W7,W8 (d)W4

Fig. 1: Wall dimensions.

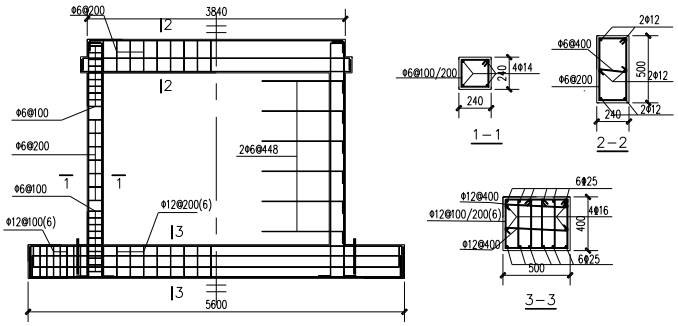

Fig. 2: Schematic diagram of specimen reinforcement.

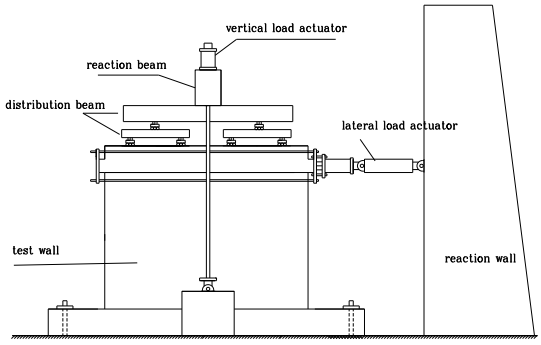

Fig. 3: Experimental setup.

The test set-up for the quasi-static reversed cyclic loadings is shown in Fig.3. Vertical load was provided by a hydraulic load actuator and distribution beam and maintained 220kN within the loading process. The magnitude of the axial load causes the compressive stress in the walls by approximately 0.25MPa. The quasi-static reversed cyclic loads were applied in plane using MTS hydraulic servo actuator step by step. Before the test wall cracked, the hydraulic servo actuator was controlled according to the magnitude of load and the load was applied in one cycle for each magnitude, while after the wall cracked, the hydraulic servo actuator was controlled according to the magnitude of lateral displacement and the load was applied in three cycles for each magnitude.

3. Test Results and Discussion

3.1. Test Observations and Crack Patterns

The initial crack of wall W1 occurred at the load of $0.85P_u$ (P_u is the shear capacity of the wall), which appeared as a inclined shear cracking at the lower corner of the wall and the tie column was cut off. When the lateral displacement attained $0.67\Delta_u$ (Δ_u is the maximum lateral displacement), the initial crack extended rapidly and formed a main shear cracking, which cut off the other tie column at the upper corner of the wall with a loud noise. The X-shape main shear cracking formed at the load of P_u and thereafter the lateral load decreased rapidly and the wall failed. In a word, wall W1 failed in a sudden and brittle way. The damage photo of wall W1 is shown in Figure 5a.

Wall W2 was retrofitted using three pairs of post-tensioned tendons. The initial crack of wall W2 occurred at the load of $0.67P_u$, which appeared as a horizontal cracking at the lower corner of the tie column. As the load increased, horizontal cracks occurred at the lower corner of the other tie column. Shear cracks occurred at the lower corner of the wall at the load of $0.89P_u$. When the load increased to $0.95P_u$, the initial horizontal cracks at the tie columns extended in opposite direction and connected into a long horizontal crack. The X-shape main shear cracking formed at the load of P_u and thereafter the lateral load began to decrease slowly. As the lateral deformation increased, new horizontal cracks and shear

cracks occurred continuously. When the lateral displacement attained Δ_u, the wall was cut into two parts along the main shear crack and the wall failed. The damage photo of wall W2 is shown in Figure 5b.

Wall W6 was retrofitted using four pairs of post-tensioned tendons. The initial crack of wall W6 occurred at the load of $0.49P_u$, which appeared as a horizontal cracking at the lower corner of the tie column. The initial shear crack occurred at the lower corner of the wall at the load of $0.89P_u$. When the load increased to P_u, the X-shape main shear cracking formed. As the lateral deformation increased, new horizontal cracks occurred on the tie columns and new shear cracks occurred on the wall continuously and the lateral load decreased very slowly. When the lateral drift attained 1/100, the lateral load remained higher than $0.85P_u$ and the bricks between the X-shape shear cracks began to be crushed, which caused the failure of the wall. The damage photo of wall W6 is shown in Figure 5f.

The other retrofitted walls had the similar failure pattern and similar failure process with the wall W2 or W6. In general, the initial crack occurred at the load of $0.6\text{-}0.7P_u$, which appeared as horizontal crack at the bottom of the tie columns. X-shape shear cracks occurred at the load of $0.9\text{-}1.0P_u$. When the lateral load began to decrease, new horizontal cracks and incline shear cracks occurred continuously and the load decreased very slowly. When the lateral load decreased to $0.85P_u$, the wall was considered failing and the cracks on the wall distributed uniformly, which shows a ductile failure pattern. The damage photos of the walls are shown in Figures 5(a-h).

a) Damage photo of wall W1

b) Damage photo of wall W2

c) Damage photo of wall W3

d) Damage photo of wall W4

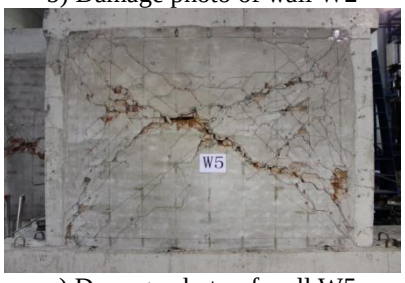

e) Damage photo of wall W5

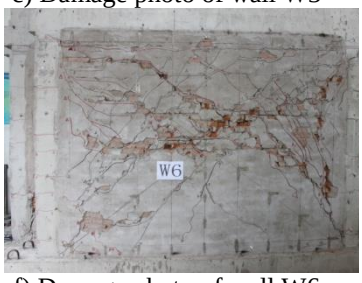

f) Damage photo of wall W6

g) Damage photo of wall W7

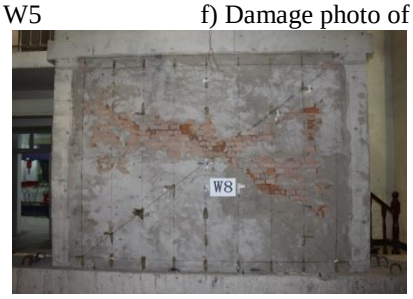

h) Damage photo of wall W8

Fig. 5: Photos of the walls at the completion of testing.

3.2. Force-Displacement Hysteretic Curves

The force-displacement hysteretic curves of the eight walls are shown in Figures 6(a-h). It can be found that the surrounding areas of the hysteretic loops of the non-retrofitted wall W1 are smaller than those of the retrofitted walls and the ductility and the energy dissipating ability of wall W1 are poor. By contrast, the surrounding area of the hysteretic loops of the retrofitted walls W2~W8 are larger and the ductility, the energy dissipating ability and the lateral load capacity are improved significantly by post-tensioned technology. It can also be found that the improvements of the shear capacity

and the ductility are depending on the magnitudes of the axial force ratio and the spacing of the prestressing tendons. In the test, wall W6 has the best ductility and wall W4 has the fullest hysteretic loops.

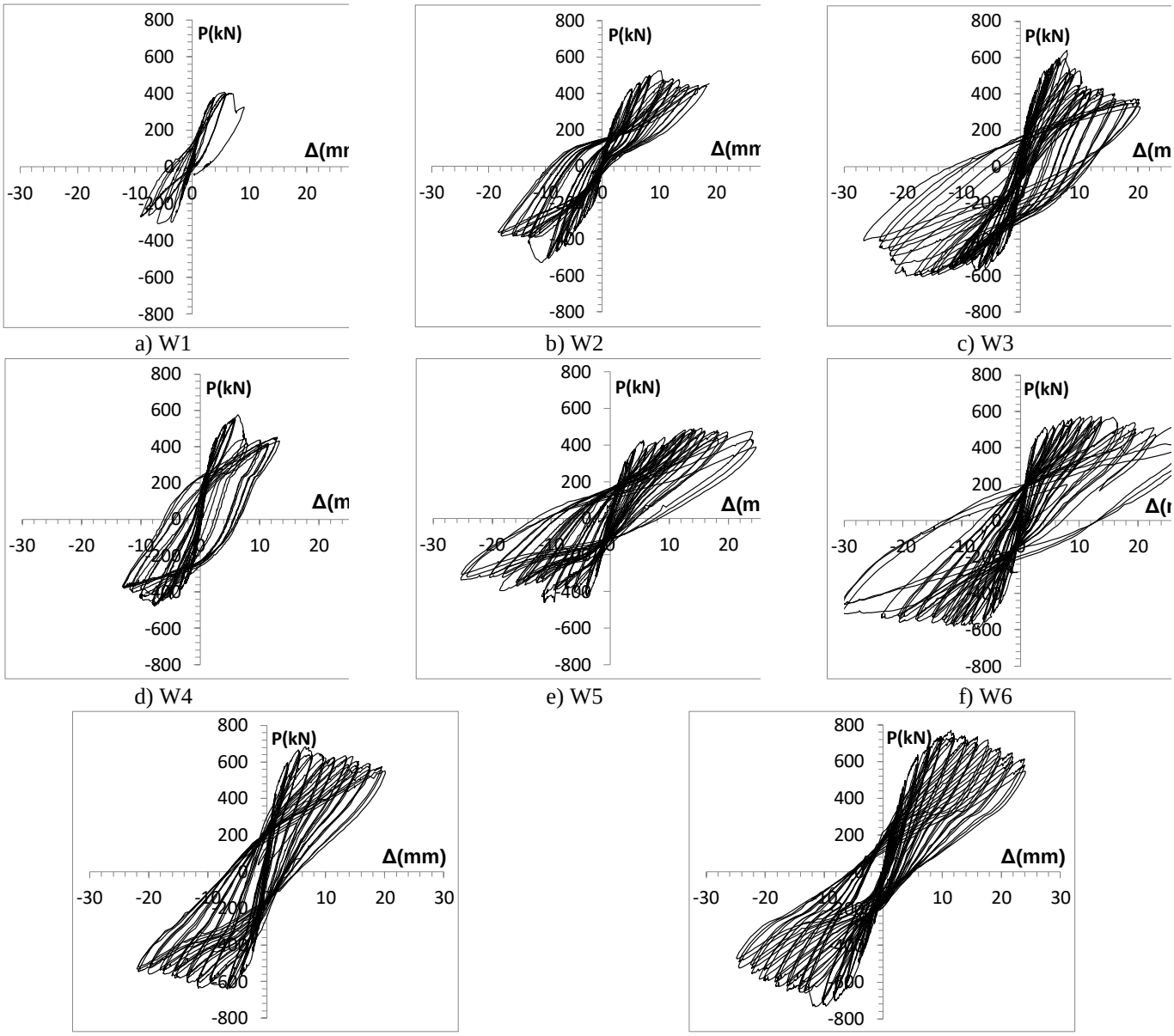

a) W1 b) W2 c) W3

d) W4 e) W5 f) W6

g) W7 h) W8

Fig. 6: Hysteretic curves of test walls.

3.3. Force-Displacement Skeleton Curve and Ductility

The force-displacement skeleton curves of the walls are shown in Figure 7 and Figure 8, vs. the spacing of tendons and the axial pressure of the walls, respectively. It can be found that the shear capacity and the deformability of clay brick walls can be significantly improved by the post-tensioned tendons. In Figure 7, the walls W2, W4 and W5 had the same axial force ratio of 0.15 due to prestress, which were retrofitted using three, five and four pairs of post-tensioned tendons, respectively. Compared with wall W1, the shear capacity and deformability of wall W2 are improved by 46% and 41%, respectively and those of wall W5 are improved by 28% and 187% and those of wall W4 are improved by 43% and 15%, respectively.

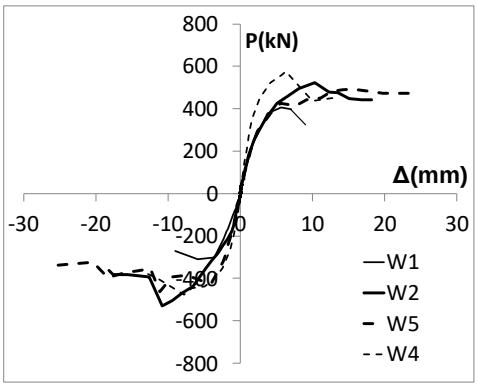

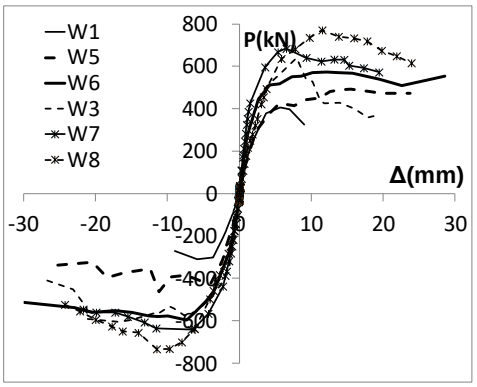

Fig. 7: P-Δ Skeleton curves vs. spacing of post-tensioned tendons Figure 8 P-Δ skeleton curves vs. axial pressure of the walls.

In Figure 8, the walls W3, W5, W6, W7 and W8 had the same spacing of 900mm between prestressing tendons, which means all these walls were retrofitted using four pairs of post-tensioned tendons. However, the axial force ratios of the walls are different, see Table 1. It can be found that the shear capacity of the wall can be greatly improved along with the improvement of the axial force ratio. Compared with wall W1, the shear capacity of wall W5, W6, W3, W7 and W8 are improved by 28%, 61%, 69%, 85% and 111%, respectively. The deformability of the retrofitted walls are also significantly improved compared with wall W1, among them the minimum increasing percentage is 24% for wall W3 and the maximum is 3.4 times for Wall W6.

The mechanical properties of the test walls are listed in Table 2. It can be seen that the ductility index of the retrofitted walls are higher than that of the non-retrofitted wall. Among the walls with the same axial pressures due to prestress and different spacing of prestressing tendons, the ductility index of wall W5(using four pairs of post-tensioned strands with spacing of 900mm)exceeds 7.32. The ductility index of wall W6 (σ_{p0}/f =0.2)exceeds 9.42, which shows the highest energy dissipating ability among all the test walls. It can also be found from the ductility index of W7 and W8 that the ductility index will decrease when the axial force ratio exceeds 0.4. But in any case, the ductility of post-tensioned retrofitted wall is better than the non-retrofitted one.

Table 2: Mechanical properties of test walls.

Wall	Yielding Load P_y (kN)	Yielding Displacement Δ_y (mm)	Shear Capacity P_u (kN)	Ultimate Displacement Δ_u (mm)	Ductility Index $\mu=\Delta_u/\Delta_y$
W1	332.9	3.55	356.7	8.80	2.48
W2	337.0	3.77	522.1	12.44	3.30
W3	437.7	2.79	604.2	10.90	3.90
W4	406.8	2.71	509.6	10.10	3.73
W5	366.8	3.45	455.9	> 25.25	> 7.32
W6	452.8	3.18	576	> 29.97	> 9.42
W7	488.3	2.59	661.5	20.09	7.76
W8	576.0	5.11	751.2	19.65	3.84

3.4. Prestressing force

To investigate the prestressing force history, the pressure sensors were set between the anchor plate and the anchorage. The prestressing stress history against the lateral load for wall W2 are shown in Figures 9(a and b) for the first group of tendons and second group of tendons, respectively. According to the experimental setup, there are 3 groups of post-tensioned tendons symmetrically arranged for wall W2. The distance from the first (or the third) group of tendons to the central axis of the tie column is 600mm, and that of the second group is 1800mm. It can be observed that the stress increment of the tendons is small before cracking and significant stress increment will occur along with the cracking process. The maximum stress increment of the first group of tendons is about 206MPa and that of the second group of tendons is about 141MPa, which shows that the stress increment of prestressing tendons near the edge of the wall is larger

than that of the tendons near the middle of the wall. The prestressing tendons near the edge of the wall play a more important role in controlling crack development.

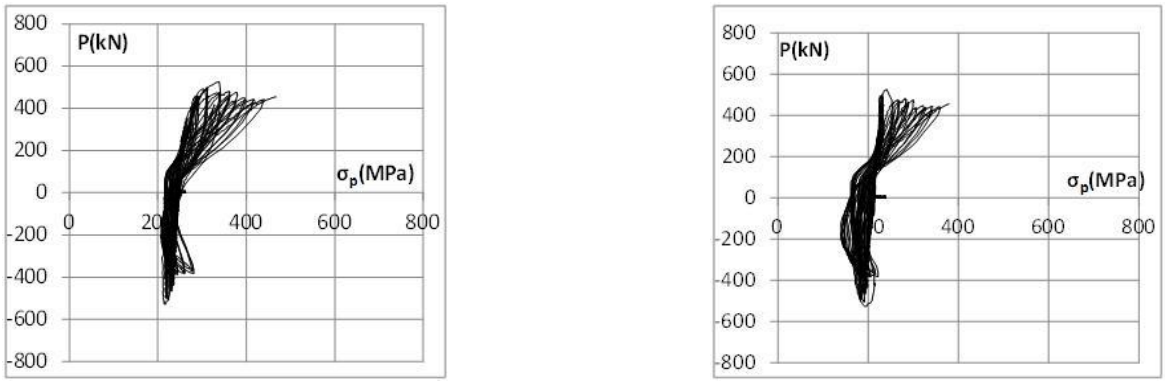

a) The first group of tendons b)The second group of tendons

Fig. 9: Prestressing stress history of wall W2.

3.5. Stiffness Degradation

The lateral stiffness degradation against the top of wall displacement is shown in Figures 10 (a and b) vs. the spacing of tendons and the axial pressure of the walls, respectively. In the figures, the Y-axis shows the ratio of the degradated stiffness K_i and the initial elastic stiffness K_1 and the X-axis shows the lateral displacement of the wall. It can be seen that compared with the non-retrofitted wall, the stiffness degradation rates of the retrofitted walls are slower. For the walls with the same axial force ratio, the stiffness degradation rate of wall using 3 and 4 pairs of post-tensioned tendons is slower than the wall using 5 pairs of post-tensioned tendons. In general, the stiffness degradation rates of all retrofitted walls have similar features and values and post-tensioned tendons can effectively enhance the after-crack stiffness of the walls and therefore play a role of second line of defense under earthquake.

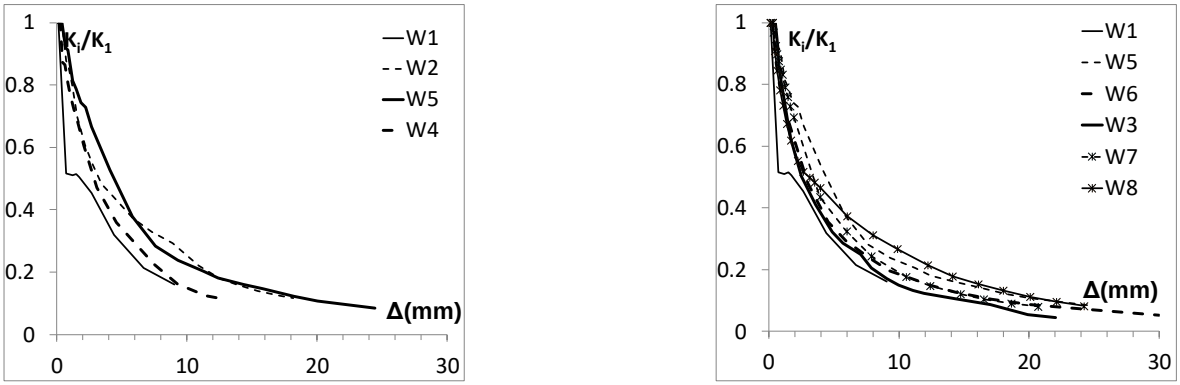

a) vs. spacing of tendons b) vs. axial pressure of walls

Fig. 10: Stiffness degradation against lateral displacement.

3.6. Energy Dissipation Ability

The energy dissipating ability of the walls can be estimated using equivalent viscous damping coefficient. The equivalent viscous damping coefficient against the top of wall displacement is shown in Figures 11 (a and b) vs. the spacing of tendons and the axial pressure of the walls, respectively. It can be seen that equivalent viscous damping coefficient increases as the walls displace laterally, which is a result of cracks friction development. The energy dissipation ability of walls can be significantly improved due to the friction between the parts of the walls on both sides of the cracks. The equivalent viscous damping coefficients of the retrofitted walls are higher than that of the non-retrofitted wall W1, which shows that the energy dissipation ability of clay brick walls can be greatly improved using the post-tensioned technology.

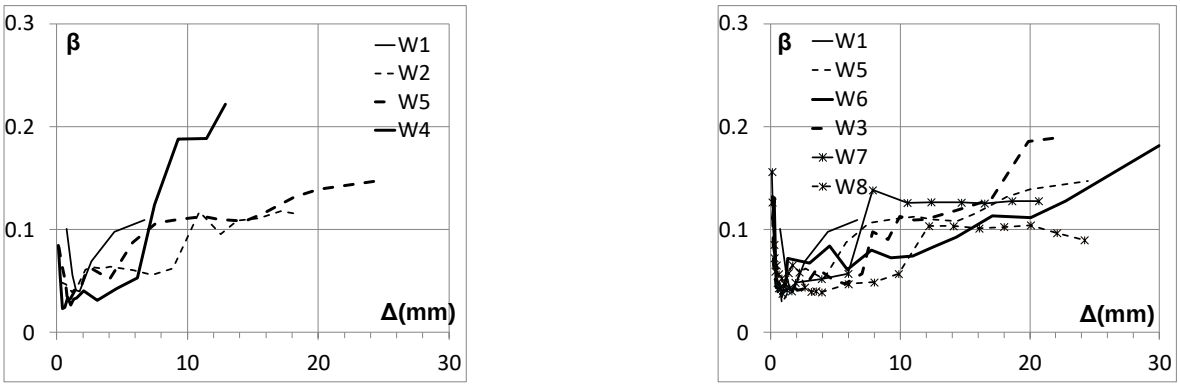

a) vs. spacing of tendons b) vs. axial pressure of walls

Fig. 11: Equivalent viscous damping coefficient against lateral displacement.

5. Conclusions

The test of eight walls subjected to quasi-static reversed cyclic loadings has validated the improvement in seismic behavior of using post-tensioned tendons to retrofit clay brick walls. The failure pattern of the retrofitted wall can be improved significantly. When the X-shape shear cracks occurred in the retrofitted wall, the lateral load begins to decrease very slowly and new horizontal cracks and incline shear cracks occurred continuously, which shows a ductile failure pattern. Meanwhile, the stress in the post-tensioned tendons will increase significantly, which shows that the post-tensioned tendons has played an effective role of second line of defense under earthquake, and as a result, the masonry building using retrofitted walls can resist high seismic forces without collapse.

The seismic capacity of the retrofitted brick masonry walls can also be improved significantly by post-tensioned technology. In the test, the increases in shear capacity of the retrofitted walls ranged from 28% to 110% higher than that of the non-retrofitted wall, and the shear capacity of the retrofitted wall increases when the magnitude of axial force ratio due to prestress force increases.

The ductility and the energy dissipation ability can also be improved greatly. The increases of displacement ductility index ranged from 33% to 280% higher than the ductility index of the non-retrofitted wall. It can also be found that the ductility index will decrease when the axial force ratio exceeds 0.4. But in any case, the ductility of post-tensioned retrofitted wall is better than the non-retrofitted one.

References

[1] M. ElGawaday, P. Lestuzzi, M. Badoux, "A review of conventional seismic retrofitting techniques for URM," *13th International Brick and Block Masonry Conference*, Amsterdam, 2004

[2] N. Mojsilovic, and P. Marti, "Load Tests on Post-Tensioned Masonry Walls," *TMS Journal*, vol. 18, no. 1, 65-70, 2000.

[3] O. A. Rosenboom, and M. J. Kowalsky, "Reversed in-plane cyclic behavior of posttensioned clay brick masonry walls," *J. Struc. Eng*., vol. 130, no. 5, 787-798, 2004.

[4] S. Chuang, Y. Zhuge, P. C. McBean, "Seismic retrofitting of unreinforced masonry walls by cable system," *3th World Conference on Earthquake Engineering*, Vancouver, Canada, 2004.

[5] P. T. Laursen, J. M. Ingham, "Structural testing of large-scale posttensioned concrete masonry walls," *J. Struc. Eng.*, vol. 130, no. 10, pp. 1497-1505, 2004.

[6] G. D. Wight, M. J. Kowalsky, J. M. Ingham, "Shake table testing of posttensioned concrete masonry walls with openings," *J. Struct. Eng*., vol. 133, no. 11, pp. 1551-1559, 2007.

[7] G. D. Wight, J. M. Ingham, and M. J. Kowalsky, "Shake table testing of rectangular posttensioned concrete masonry walls," *ACI Struct. J*., vol. 103, no. 4, pp. 587-595, 2006.

[8] N. Ismail, P. Laursen, J. M. Ingham, "Out-of-plane testing of seismically retrofitted URM walls using posttensioning," in *Proceedings of The AEES Conference*, Newcastle, Australia, 2009.

[9] G. D. Wight, J. M. Ingham "Tendon stress in unbounded posttensioned masonry walls at nominal in-plane strength," *J. Struct. Eng.*, vol. 134, no. 6, pp. 938-946, 2008.

[10] G. D. Wight, J.M. Ingham, A. R. Wilton, "Innovative seismic design of a post-tensioned concrete masonry house,"

Canadian Journal of Civil Engineering, vol. 34, no. 11, pp. 1393-1402, 2007.
[11] N. Ismail, P. T. Laursen, A. E. Schultz, J. M. Ingham, "Cyclic out-of-plane behavior of post-tensioned clay brick masonry," *11th North American Masonry Conference*, Minneapolis, Minnesota, 2011
[12] J. R. B. Popehn, A. E. Schultz, "Influence of imperfections on the out-of-plane flexural strength of post-tensioned masonry walls," *Construction and Building Materials*, vol. 41, pp. 942-949, 2013.
[13] R. Ma, L. Jiang, M. He, C. Fang, F. Liang, "Experimental investigations on masonry structures using external prestressing techniques for improving seismic performance," *Engineering Structures*, vol. 42, pp. 297-307, 2012.
[14] L. Hang, H. Shaofeng, "Test & Analysis on Seismic Behaviors of Brick Walls Retrofitted with Post-tensioned Tendons," *Earthquake Resistant Engineering and Retrofitting*, vol. 35, no. 5, pp. 71-78, 2013. (in Chinese)
[15] L. Hang, L. Chunguang, Hua Shaofeng, "Research and application of seismic strengthening technology to existing masonry structures in villages and small towns," *World Earthquake Engineering*, vol. 30, no. 3, pp. 156-162, 2014. (in Chinese)
[16] China Ministry of Construction. Code for design of masonry structures (GB50003-2011), Beijing (China); China Architecture & Building Press, 2011.